PL-TR-97-2030

REGIONAL WAVE PROPAGATION CHARACTERISTICS IN THE MIDDLE EAST AND SOUTHERN ASIA

Richard Rapine
James Ni
Tom Hearn

New Mexico State University
Department of Physics
Las Cruces, NM 88003-8001

October 1996

Scientific Report No. 1

DEPARTMENT OF ENERGY
Office of Non-Proliferation
and National Security
WASHINGTON, DC 20585

19970606 132

PHILLIPS LABORATORY
Directorate of Geophysics
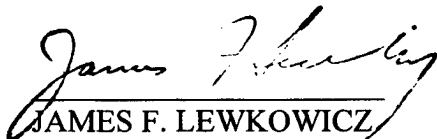AIR FORCE MATERIEL COMMAND
HANSCOM AFB, MA 01731-3010

DTIC QUALITY INSPECTED 1

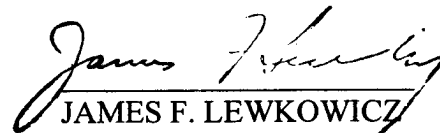This technical report has been reviewed and is approved for publication.

JAMES F. LEWKOWICZ
Alternate Contract Manager
Earth Sciences Division

JAMES F. LEWKOWICZ
Director
Earth Sciences Division

REPORT DOCUMENTATION PAGE

1. AGENCY USE ONLY (Leave blank)	2. REPORT DATE October, 1996	3. REPORT TYPE AND DATES COVERED Scientific Report No. 1

4. TITLE AND SUBTITLE	5. FUNDING NUMBERS
Regional Wave Propagation Characteristics in the Middle East and Southern Asia	F19628-95-K-0009 PE69120H PR DENN TAGM WUAH
6. AUTHOR(S) Richard Rapine, James Ni and Tom Hearn	

7. PERFORMING ORGANIZATION NAME(S) AND ADDRESS(ES)	8. PERFORMING ORGANIZATION REPORT NUMBER
New Mexico State University Department of Physics Las Cruces, NM 88003-8001	

9. SPONSORING/MONITORING AGENCY NAME(S) AND ADDRESS(ES)	10. SPONSORING/MONITORING AGENCY REPORT NUMBER
Phillips Laboratory 29 Randolph Road Hanscom AFB, MA 01731-3010 Contract Manager: Delaine Reiter/GPE	PL-TR-97-2030

11. SUPPLEMENTARY NOTES

This research was sponsored by Department of Energy, Office of Non-Proliferation & National Security, Washington, D.C. 20585

12a. DISTRIBUTION/AVAILABILITY STATEMENT	12b. DISTRIBUTION CODE
Approved for public release; distribution unlimited	

13. ABSTRACT (Maximum 200 words)

The regional seismic waves Pn, Sn and Lg were used to map lateral variations of attenuation in the crust and upper mantle. Propagation efficiencies of Sn and Lg were qualitatively analyzed by ranking their amplitudes relative to the P-wave coda. Efficient Sn propagation is observed in the Tien Shan, Tarim Platform, southern Tibet, Yangzi Paraplatform and Sino-Korean Platform. We have confirmed previous studies by finding a lack of Sn transmission in north-central Tibet, the Ryukyu and Japan Arcs, Burma and the Baikal Rift. An important observation, which has not been previously reported, is that Sn does not propagate across Mongolia. The elimination of Sn and recent volcanism in north-central Tibet and Mongolia suggest that there is partial melt in the upper most mantle beneath those regions. High frequency Lg waves propagate efficiency for most of China, Indochina and Mongolia. Lg signals are attenuated within central Tibet as well as along its southern boundary.

14. SUBJECT TERMS	15. NUMBER OF PAGES 42
Crustal structure, Seismic studies, Middle East, Far-East, Tibetan Plateau	16. PRICE CODE

17. SECURITY CLASSIFICATION OF REPORT	18. SECURITY CLASSIFICATION OF THIS PAGE	19. SECURITY CLASSIFICATION OF ABSTRACT	20. LIMITATION OF ABSTRACT
Unclassified	Unclassified	Unclassified	SAR

Table of Contents

List of Illustrations

List of Tables

1. Introduction

China and its surrounding regions are one of the most seismically active intracontinental regions on Earth. The active seismicity, especially in western China, is associated with the late Cenozoic continental collision between the Indian and Eurasian plates. This collision not only created the world's largest mountain system and plateau, the Himalayas and Tibetan Plateau, but also reactivated old mountain belts such as the Tien Shan and Altay Mountains (Molnar and Tapponnier, 1975). Prior to the Himalayan orogeny, the tectonic framework of China evolved through a series of collisional events among continental blocks and island arcs since the Cambrian age (e.g., Sengor, 1987; Yin and Nie, 1996). Microcontinents and island arcs in the Tethyan oceans have also contributed significantly to the formation of the Asian continent. These continental and oceanic fragments include the Sino-Korean block, Yangzi block, Mongolian island arcs, Tarim block, Qiangtang block and Lhasa block (Figure 1). The continental blocks, consisting of metamorphic basement rocks as old as the early Archean (Liu *et al.*, 1992), are not significantly deformed. In contrast, the fold belts that lie between the ancient blocks are highly deformed and exhibit very different physical properties than the crust of the old cratons. Through subduction during the Paleozoic, Mesozoic and Cenozoic time, much of the upper mantle beneath Mongolia, Inner Mongolia, Tibet and Southeast China has been enriched by residual melts and metasomatizing fluids. The modified mantle may have been hydrated and hence, was probably buoyant relative to the underlying mantle. The residence time for this less dense mantle could have been a very long time (Anderson, 1995). This buoyant mantle, when subjected to either extensional or compressional strain energy during a later tectonic event, could be in an extensive state of partial melt. The seismic phenomenon associated with a partially melted uppermost mantle is the absence of high-frequency Sn waves.

The tectonic history of China also plays an important role in Lg attenuation. Major changes in the crustal waveguide and thickness as well as partial melt in the crust can be linked to present as well as previous tectonic orogenies and these features may cause the blockage of Lg. It is a well known phenomenon that Lg is weakened by scattering and crustal heterogeneities (e.g., Knopoff *et al*, 1973; Bouchon, 1982; Kennett, 1985), however, it may not be completely extinguished by these effects. Husebye and Ruud (1996) have shown that the attenuation of crustal Lg waves in the North Sea grabens is directly related to the intrinsic attenuation of a partially melted crust. Therefore, it is likely that a combination of
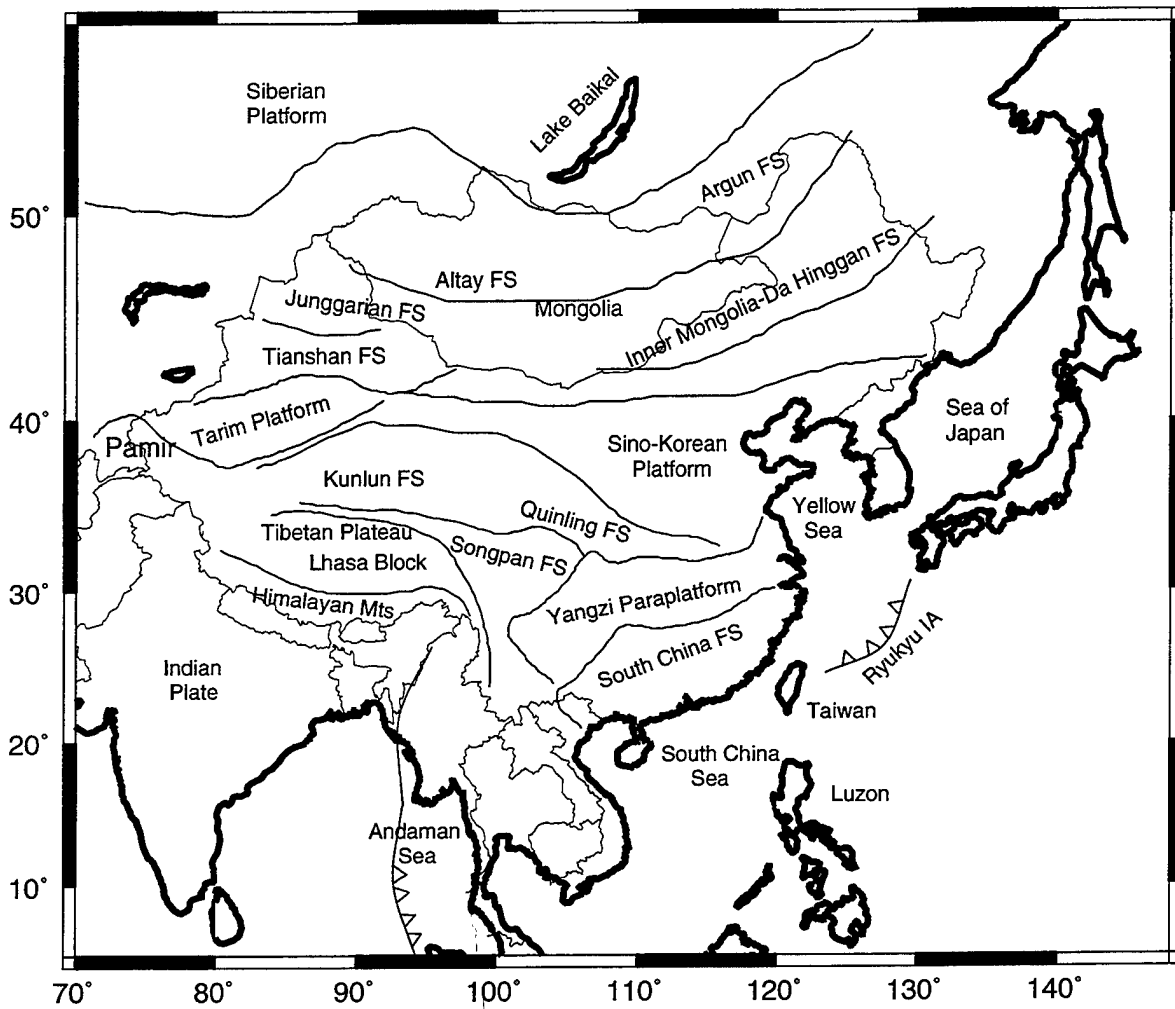
Figure 1. A simplified tectonic map of China and its surrounding regions. Dark lines separate the major tectonic provinces in the region. Triangles represent the direction of oceanic sub-duction. (FS-Fold System, IA-Island Arc, MTS-Mountains) (modified from Huang et al., 1987; Huang, 1979; Coleman, 1989; Chinese Academy of Geological Sciences, 1976)

scattering and partial melt in the crust may explain the complete elimination of the Lg arrival on regional seismograms.

Since Lg and Sn wave propagation characteristics are diagnostic of crust and upper mantle properties, respectively, we visually inspect how these waves propagate in China and its surrounding regions to better understand the active tectonics of the region. In addition, we examine the relevance of Sn and Lg propagation efficiencies to the application of discriminants for nuclear test monitoring. Previously, various high-frequency waves, such as Sn and Lg, have been used to develop short-period discriminants (e.g. Pomeroy et al., 1982; Taylor et al., 1989). For example, Pg and Lg amplitude ratios are an indication of the relative amount of compressional and shear-wave energy radiated from a seismic source. Low Pg/Lg ratios are often associated with earthquakes because its source occurs along a planar fault and radiates significant amounts of shear energy relative to compressional energy; high Pg/Lg ratios are usually associated with explosions because its source radiates more compressional than shear energy. However, these phases propagate in different parts of the earth and the regional geology along a path can alter the relative strength of the signals. This implies that a discriminant that works effectively in the western United States may not be effective in certain regions of China. Therefore, the significance of this study is two-fold. First, it is important to understand how the geology of a region affects Sn and Lg phase propagation and where attenuation of these phases occurs. Second, this study will determine which phases or combination of phases may be useful as discriminants in China for a Comprehensive Test Ban Treaty (CTBT).

This report will examine, classify and map the propagation efficiencies of high-frequency seismic waves at regional distances in China. Emphasis is focused on where these waves are attenuated or blocked. This information will be integrated with our knowledge of what causes efficient or inefficient propagation. Then we will discuss how the past and recent tectonics of China have influenced the propagation characteristics. Finally, we will determine the applicability of Sn and Lg phases to nuclear discrimination in the region. A significant result of this research shows that a ratio method which uses short-period Sn would not be a useful discriminant in China since it is attenuated or weakened in a majority of the regions.

3

2. Data

The data for this study were digitally recorded by the Chinese Digital Seismic Network (CDSN) and retrieved through the Incorporated Research Institutions for Seismology - Data Management Center (IRIS-DMC). The CDSN network (Figure 2), which began operation in October 1986, consists of 11 three-component, broadband stations spread geographically throughout China. Data from two stations of the Global Seismic Network (GSN) were also included in our study. Table 1 summarizes the information about all 13 seismic stations we have studied. The digital, broadband data were collected in event-triggered mode at a sampling rate of 20 samples per second. All the stations were equipped with either Streckseisen Model STS-1, STS-1/VBB or STS-2/VBB three-component sensors. The amplitude response of the sensors was flat between 0.1 and 10 Hz. Event origin times and locations were taken from the Preliminary Determination of Epicenters (PDE) catalogs distributed by the U.S. Geological Survey (USGS). Our objective was to look at regional, crustal seismic events with a high signal-to-noise ratio. Therefore, the criteria for our database were chosen such that we extracted all events having epicentral distances between 2^0 and 20^0, the complete range of azimuths, body wave magnitudes greater than 4.3 and depths less than 50 km. The data presented in these results are for events with epicentral distances between 2^0 and 15^0.

3. Method of Analysis

In this study, we will investigate the propagation efficiencies of the high-frequency regional phases Pn, Sn and Lg. Pn is the first arrival on regional seismograms for distances greater than about 3^0. Pn wave transmission has been modeled as whispering gallery waves trapped in a waveguide comprised of a high-velocity mantle lid with a low-velocity zone beneath it (Menke and Richards, 1980). The shear-wave counterpart of Pn in the mantle is Sn. The Sn phase has been studied in terms of normal modes of Love waves with the mantle lid acting as a waveguide (Stephens and Isacks, 1977). Due to the shear-wave nature of Sn, it is diagnostic of lateral variations of attenuation caused by heating and partial melt in the upper mantle. Therefore, we have emphasized our efforts on determining the transmission efficiency of Sn rather than Pn. Efficient propagation of Sn has usually been observed in the uppermost mantle beneath stable shield regions (e.g., Bath, 1966; Brune and Dorman, 1963).
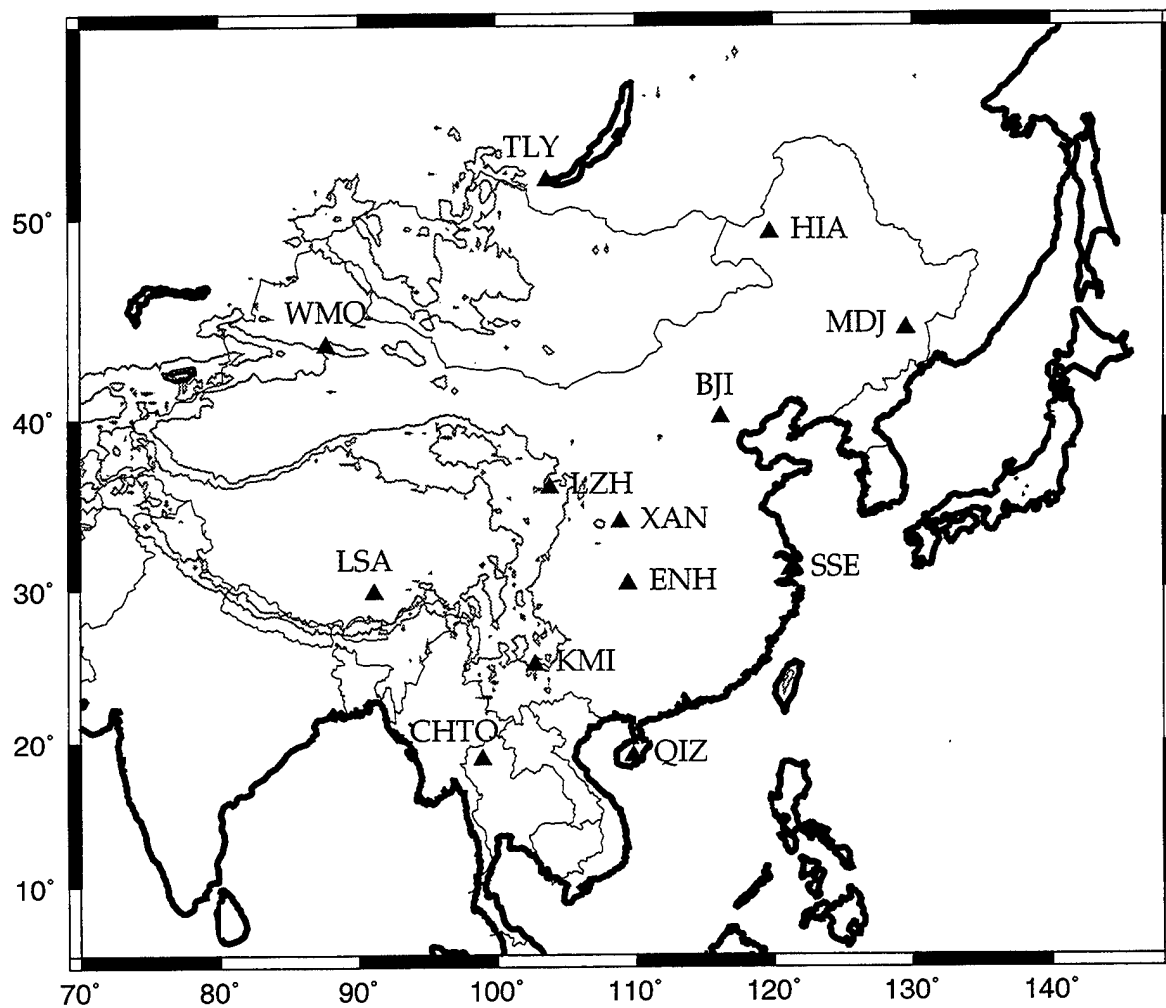
Figure 2. A station location map for the Chinese Digital Seismic Network (CDSN) stations we investigated. Black triangles represent station locations. Gray lines represent 2000m and 4000m elevation contours. There are two Global Seismic Network (GSN) stations we have also included - TLY (Lake Baikal) and CHTO (Thailand). (see Table 1 for complete listing)

Table 1

Summary of the CDSN and GSN stations under study. The network name and station name, their geographic locations and the period of data we obtained for them are listed.

Network Name	Station Name	Station Location	Years
CDSN	BJI	Beijing, China	1988 - 1994
GSN	CHTO	Chiang Mai, Thailand	1992 - 1995
CDSN	ENH	Enshi, China	1989 - 1994
CDSN	HIA	Hailar, China	1988 - 1994
CDSN	KMI	Kunming, China	1988 - 1994
CDSN	LSA	Lhasa, China	1991 - 1994
CDSN	LZH	Lanzhou, China	1988 - 1994
CDSN	MDJ	Mudanjiang, China	1988 - 1994
CDSN	QIZ	Qiongzhong, China	1992 - 1994
CDSN	SSE	Shanghai, China	1989 - 1994
GSN	TLY	Talaya, Russia	1991 - 1994
CDSN	WMQ	Urumqi, China	1988 - 1994
CDSN	XAN	Xi'an, China	1992 - 1994

Lg is a high-frequency, large amplitude wavetrain seen at regional distances from 2^0 to 25^0. Lg travels in a group velocity window of 3.7-3.2 km/s and is indicative of stable shield regions. Lg was first interpreted as a higher-mode shear-wave propagating in a crustal waveguide consisting of a granitic layer (Press and Ewing, 1952). Press and Ewing (1952) also revealed that Lg does not propagate across paths with more than 100 km of oceanic crust. Numerical modeling techniques of elastic wave propagation in a vertical heterogeneous crust have shown Lg as a superposition of S-waves that are multiply reflected within the crust and incident on the Moho at a post-critical angle (Bouchon, 1982). Lg propagation is sensitive to crustal thickness and waveguide variations (e.g., Ruzaikin et al., 1977; Campillo, 1987), however, Lg may not be eliminated completely by these features alone. Blockage of Lg is observed for paths across the North Sea graben structures but crustal thinning is insufficient for explaining the absence of Lg (Husebye and Ruud, 1996). To model Lg blockage to the extent seen on seismograms, a very low Q crust of the order of 100 at 2 Hz is needed for the graben crust. The significance of Lg to this study then is that it provides information about the average shear-wave velocity and attenuation of shear energy of the crust along its path.

The propagation characteristics of Pn, Sn and Lg were used to constrain structure and provide insights into the tectonic processes in China and its adjacent regions. Previous studies (e.g., Ruzaikin et al., 1977; Kadinsky-Cade et al., 1981; Ni and Barazangi, 1983; Rodgers et al., 1997) analyzed short-period analog seismograms to qualitatively characterize broad tectonic provinces and subprovinces in terms of either efficient or inefficient Pn, Sn and Lg propagation. We have used a similar empirical approach for documenting the efficiencies of observed regional phases. Over 7000 digital, broadband seismograms were examined in total from all of the stations. All three components of the seismograms were bandpass filtered between 0.5-5.0 Hz. The high-frequency content of Sn and Lg signals varied between 0.5-3.0 Hz from station to station. The instrument responses were not taken out of the data so all data were analyzed as raw velocity seismograms. P-wave arrivals were manually picked only on the vertical component. We used a 8.2-6.0 km/s group velocity window to pick Pn and Pg. Sn and Lg were picked manually on the horizontal transverse components. A group velocity window of 4.7-4.3 km/s was used for picking Sn and a 3.7-3.2 km/s velocity window was used for picking Lg. The propagation efficiencies of Sn and Lg were ranked according to their amplitudes relative to the P-wave coda amplitude. Sn and Lg amplitudes greater than the amplitude of the P coda were classified as efficient. Sn and Lg amplitudes approximately one-half the amplitude of the P coda or less were

classified as inefficient. No Sn or Lg is specified when neither Sn nor Lg is observed above the noise level of the seismogram. At times for short epicentral distances (< 6$circ$), the presence of a Pg wavetrain with frequencies comparable to Sn made it difficult to determine the presence or absence of Sn. Therefore, when Pg obscured the seismogram at the expected arrival time of Sn and no obvious Sn energy existed on the seismogram, we classified Sn as not observed. Examples of regional, broadband seismograms have been provided in Figures 3 and 4. Figure 5 shows seismograms of nuclear explosions from the Semipalatinsk and Lop Nor test sites recorded at WMQ and TLY, as well as local earthquakes in the Lop Nor area. Figure 6 is a map of the event locations from the seismograms of Figure 5.

4. Results

4.1 Regional Sn Propagation in China

The propagation efficiencies of the regional phase Sn are ranked as efficient, inefficient and not observed and are mapped in Figures 7-9, respectively. The maps clearly show that there is a large variation in the transmission efficiency of Sn in China. We have examined the differences in the propagation efficiencies through the diverse tectonic provinces and have summarized them on a region to region basis. As seen on seismograms recorded at station LSA (Figure 3, Seismograms A and B), Sn propagates efficiently across the Himalayas and throughout southern Tibet. However, the upper mantle beneath north-central Tibet severely attenuates the Sn phase. Seismogram C in Figure 3 shows no Sn energy from paths crossing the north-central portion of the plateau. This region of poor Sn propagation was observed earlier by Ni and Barazangi (1983) and McNamara et al. (1995). For those ray paths propagating across the eastern portion of Tibet and the Songpan Fold System (FS), Sn waves are attenuated on data recorded at ENH (Seismogram D).

The Tien Shan Fold System and Tarim Platform in western China allow mostly efficient Sn propagation (Figure 7). An event recorded at WMQ, which shows efficient Sn transmission across the Tarim Platform, is provided in Seismogram E. Ray paths originating from earthquakes in the Kunlun Fold System show both efficient and inefficient Sn as observed at LZH and WMQ (Figures 7 and 8). Seismogram F, from LZH, is a waveform recording efficient Sn from the Kunlun FS through the Qaidam Basin. Seismogram G records inefficient Sn at
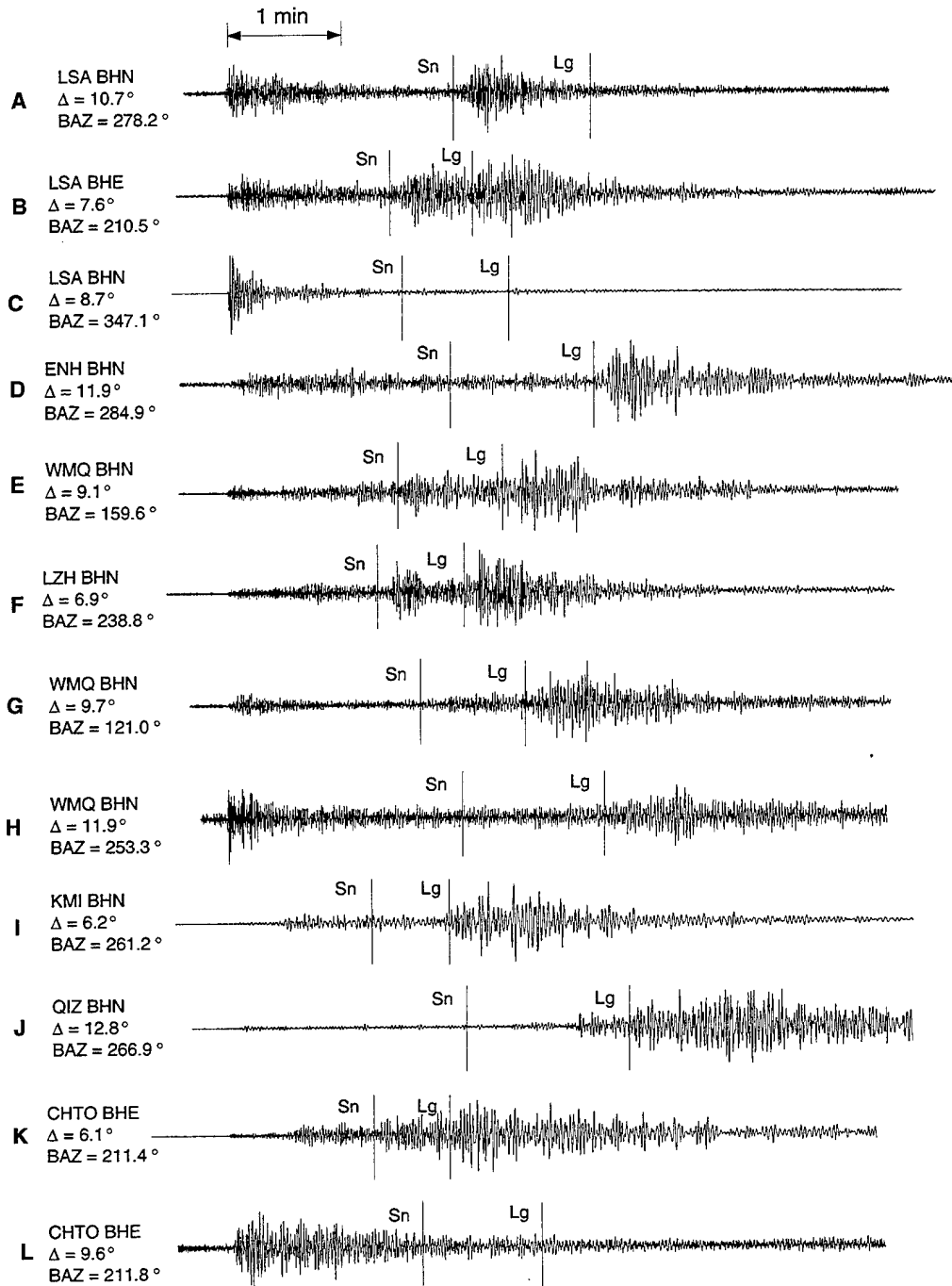
Figure 3. Representative broadband seismograms from CDSN and GSN stations. The waveforms are aligned according to the Pn phase. Verticle bars indicate the approximate arrival times of Sn and Lg, corresponding to 4.5 km/s and 3.5 km/s, respectively. The waveforms represent raw velocity seismograms and have been bandpass filtered (0.5-5.0 Hz).

9
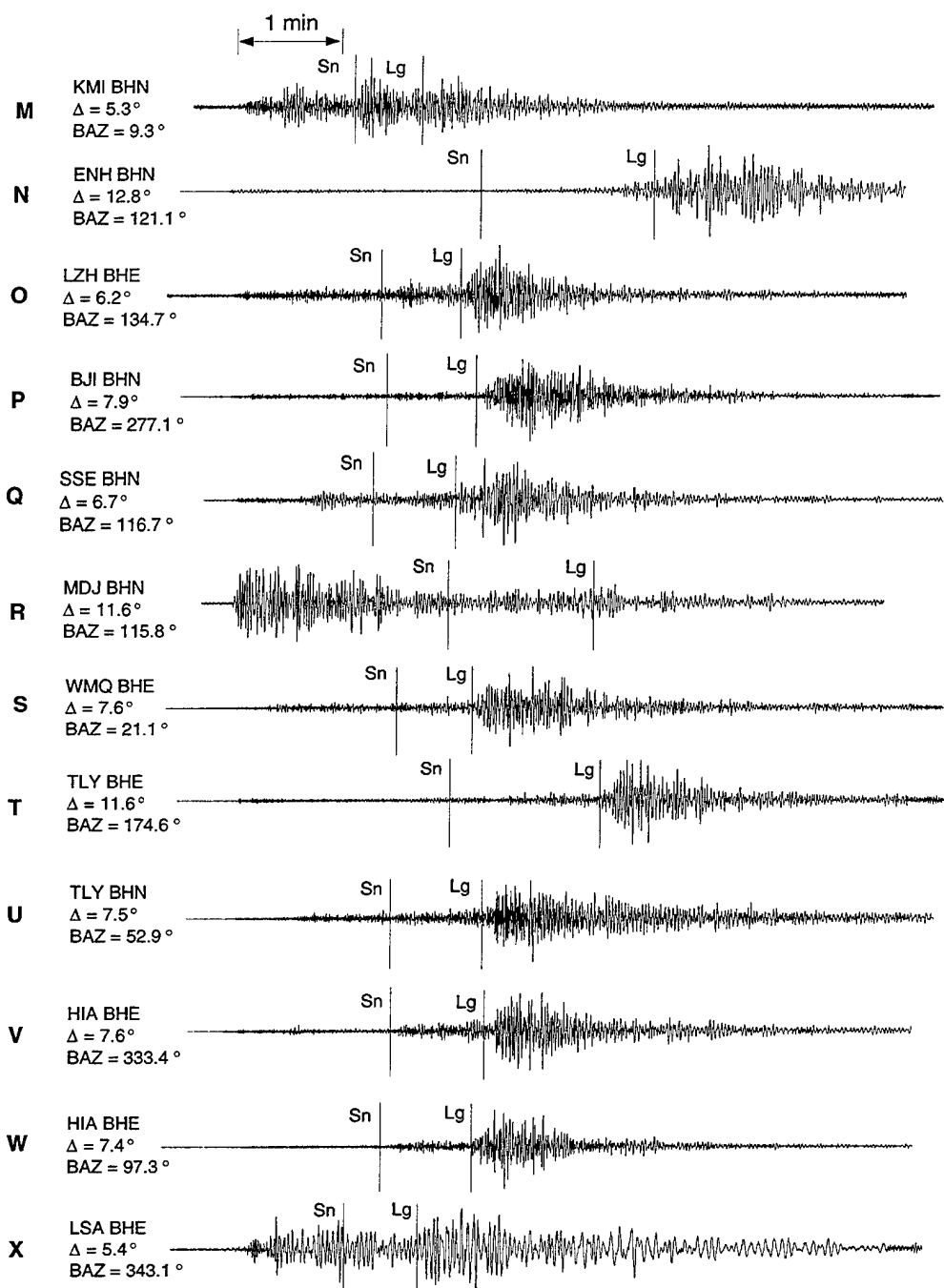
Figure 4. More seismograms from CDSN and GSN stations, same as Figure 3.
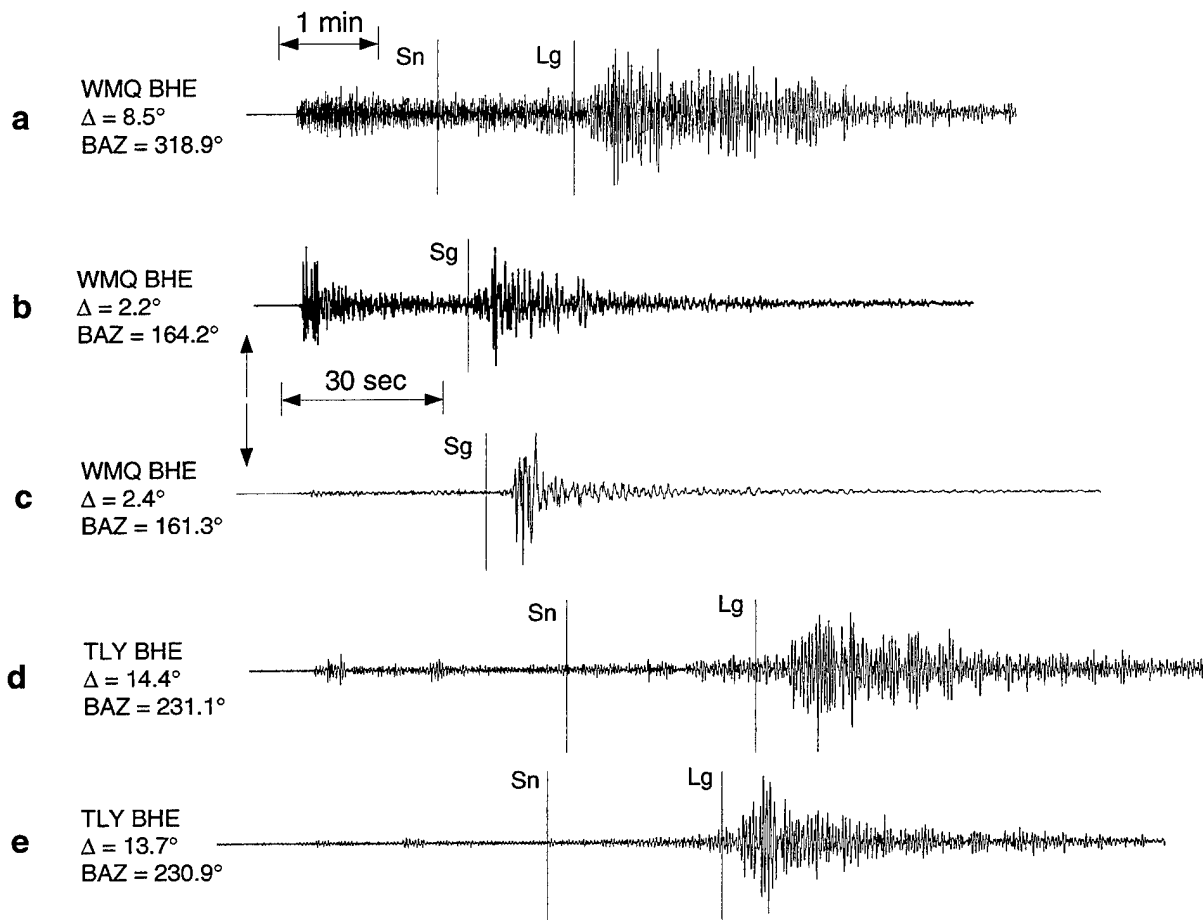
Figure 5. Seismograms a and b are nuclear explosion signals recorded at station WMQ. Seismogram a is from the test site at Semipalatinsk and Seismogram b is from the Chinese Lop Nor test site. Seismogram c is an earthquake located near Lop Nor and recorded at WMQ. Seismograms d and e are a nuclear explosion and earthquake from the Lop Nor area recorded at TLY, respectively. The vertical bar in Seismograms b and c represent Sg because of the short distances.
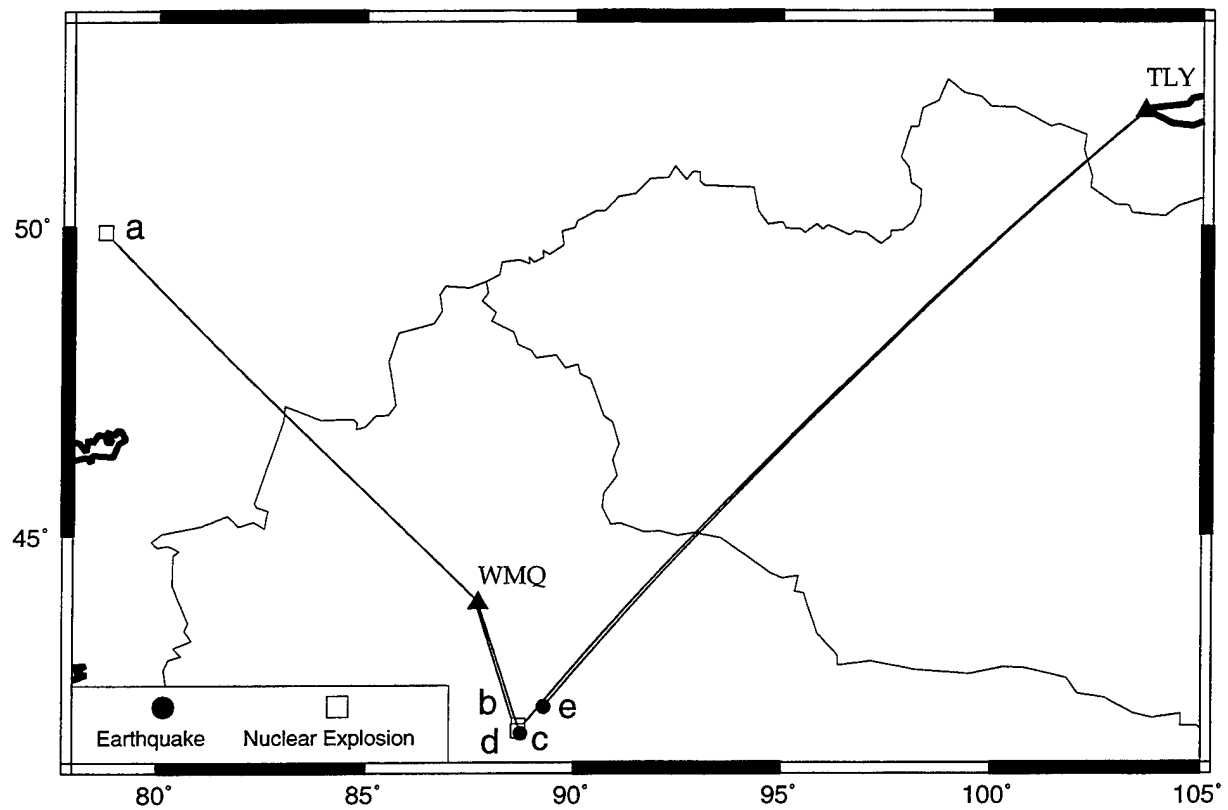
Figure 6. A map of station-event paths for nuclear explosions and earthquakes in the Lop Nor test site region and from the Semipalatinsk test site. Small letters represent locations of the seismic events depicted on seismograms from Figure 5.
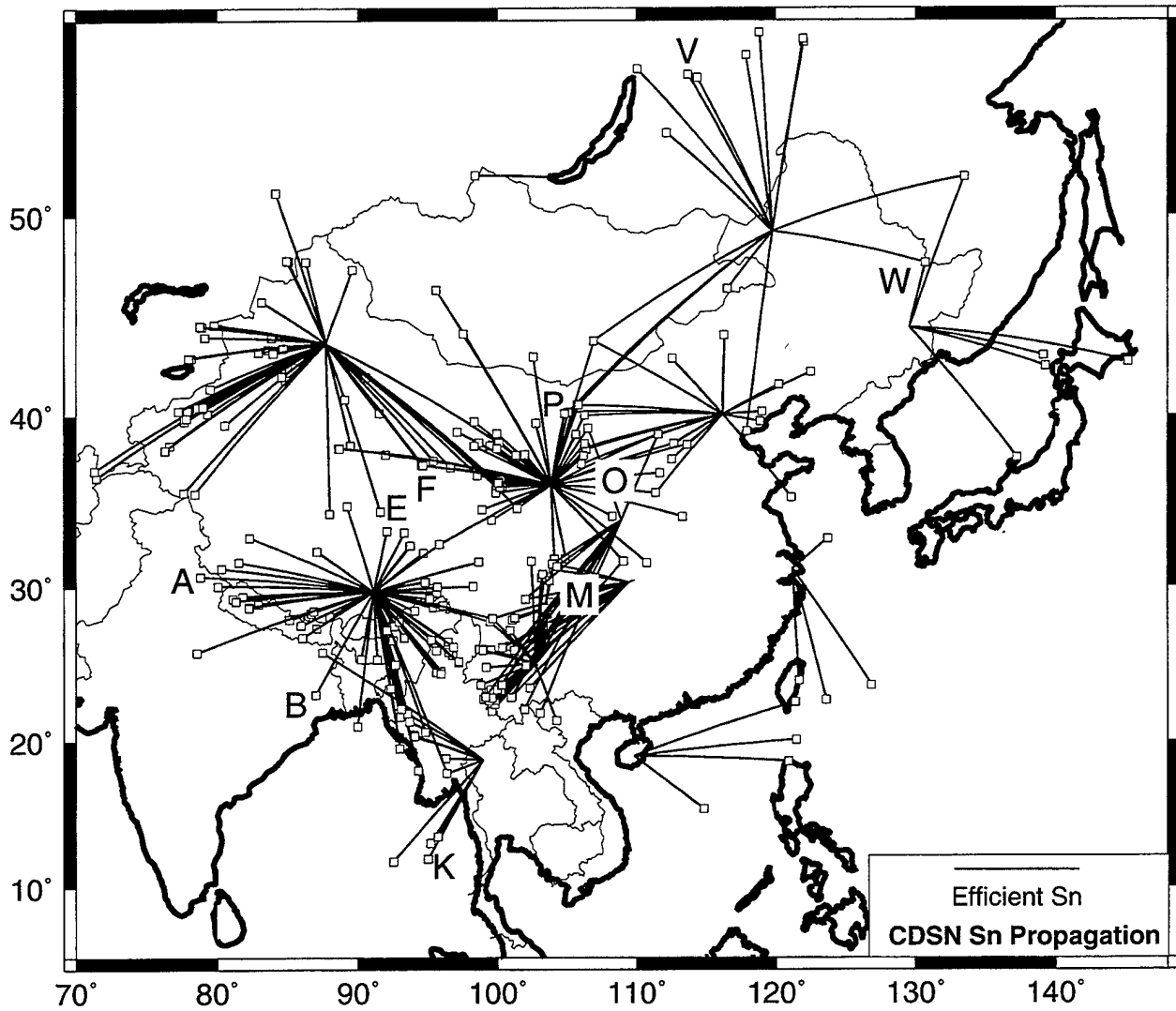
Figure 7. A map of efficient Sn propagation paths in China. The squares represent seismic events. The solid lines depict efficient station-event paths in the regions of study. All paths have epicentral distances between 2^0 and 15^0 and all events are less than 50 km deep with body wave magnitudes greater than 4.3. Capital letters represent letters represent locations of the earthquakes depicted on seismograms from Figure 3 and 4.

13

Figure 8. A map of inefficient Sn propagation paths in China. Dashed lines represent inefficient station-event paths.

Figure 9. A map depicting the station-event paths where no Sn phase was observed or where Sn was severely attenuated. For this case, propagation paths are represented by dotted lines.

WMQ from the same area. There are discrepancies in the data from earthquakes located in the Pamirs recorded at WMQ. While Sn is mostly inefficient or not observed in the region (Figures 8 and 9), there are a few paths where Sn is efficient (Figure 7). Seismogram H is a typical example of no Sn from a Pamir earthquake. There could be several reasons for the discrepancies in the Sn propagation efficiencies. The efficient Sn could be from sub-crustal earthquakes with mislocated depths, or perhaps the ray paths for Sn were deep enough to avoid shallow upper mantle melt or heterogeneities in western Tien Shan.

Sn is attenuated through the Songpan Fold System, part of the north-central Tibetan Plateau and Burma region (Figure 9). Data from this region was recorded by stations LSA, LZH, XAN, ENH, KMI and CHTO. Seismogram I from KMI with a propagation path across Burma shows no Sn phase. The continental extension of the Andaman back-arc into Burma does not transmit Sn (Figure 9), which was noted previously by Molnar and Oliver (1969). Seismogram J at QIZ shows poor Sn propagation beneath Indochina. Further south in the Andaman Sea, earthquakes located on the northeast side of the oceanic ridges (Seismogram K) show efficient Sn, while those events to the southwest and away from the ridges show no observed Sn (Seismogram L).

For a ray path entirely within the western Yangzi Paraplatform, Sn is mostly efficient (Seismogram M). Sn is attenuated when it passes through the South China Fold System from Taiwan to station ENH (Seismogram N). In central China, efficient Sn is observed for propagation paths through the Quinling Fold System to LZH (Seismogram O). For ray paths under the Sino-Korean Platform, Sn transmission is efficient (Seismogram P). Sn waves traveling west of the Ryukyu arc under the continental margin to SSE are efficient although not emergent (Seismogram Q). Attenuation of Sn by the mantle between the Japan Arc and Manchuria is observed at MDJ (Seismogram R).

A new observation concerning the Sn regional phase in Asia is that it does not propagate efficiently beneath the Mongolian Plateau. Seismograms from stations in Russia (TLY) and China (WMQ and BJI) show no Sn arrival for propagation paths traversing the plateau (Figure 9, Seismograms S and T). For ray paths crossing the long of axis of the Baikal Rift to station TLY, no Sn phases are detected (Seismogram U). In northeast China at station HIA, Sn is observed for a path propagating through the Siberian Platform and Argun Fold System

16

(Seismogram V). Paths in the Inner Mongolia/Da Hinggan region show Sn energy at HIA (Seismogram W).

Data from three nuclear explosions recorded at WMQ and TLY, two from Lop Nor and the other from Semipalatinsk, are provided in Figure 5 (Seismograms a, b, and d). Figure 6 shows a map of the locations of these nuclear explosions and earthquakes. The waveforms from these explosions have a high-frequency content but no observed Sn phase. Seismogram c is a waveform of an earthquake with a similar backazimuth and epicentral distance as the Lop Nor explosion (Seismogram b) at WMQ. The earthquake exhibits more long-period energy than the nuclear explosion. Sn and Lg signals on Seismograms b and c arrive very close together and may be interpreted as Sg for the Lop Nor seismic events because of the shortness of the station-event path (~2-3^0). Seismogram e is an earthquake recorded at TLY with an epicenter nearby Lop Nor. Sn is not observed for either the earthquake or the explosion (Seismogram d) at TLY. It has been stated earlier that Sn does not propagate across Mongolia/Altay Fold System for any seismic event.

4.2 Regional Lg propagation in China

The results of this Lg study will be summarized on a region to region basis in a manner similar to the Sn results. Lg wave station-event paths are mapped according to their efficiency in Figures 10-12. Efficient Lg is observed throughout most regions in China (Figure 10). The major regions of Lg blockage are the inner regions and southern boundary of the Tibetan Plateau and paths across oceanic crust (Figure 12). Seismogram C is an earthquake from northern Tibet which shows that Lg is completely eliminated at LSA. For a ray path parallel to the strike of the Himalayas from India, Lg is not observed (Seismogram A). However, for an event with a southern backazimuth (perpendicular to the strike of the Himalayas), Lg is efficient (Seismogram B). Inefficient and efficient propagation paths for Lg are observed within the Tibetan Plateau for epicentral distances less than 6^0 from LSA (Seismogram X). This result confirms the previous observations of McNamara et al. (1996), who saw Lg energy for events recorded within the plateau out to 600-700 km. Other significant features of Lg blockage and attenuation in southern and central Tibet, such as scattering and Lg Q, have been characterized in previous studies (e.g., Ruzaikin et al., 1977; Ni and Barazangi, 1983; McNamara et al., 1996; Reese and Ni, 1996).

17

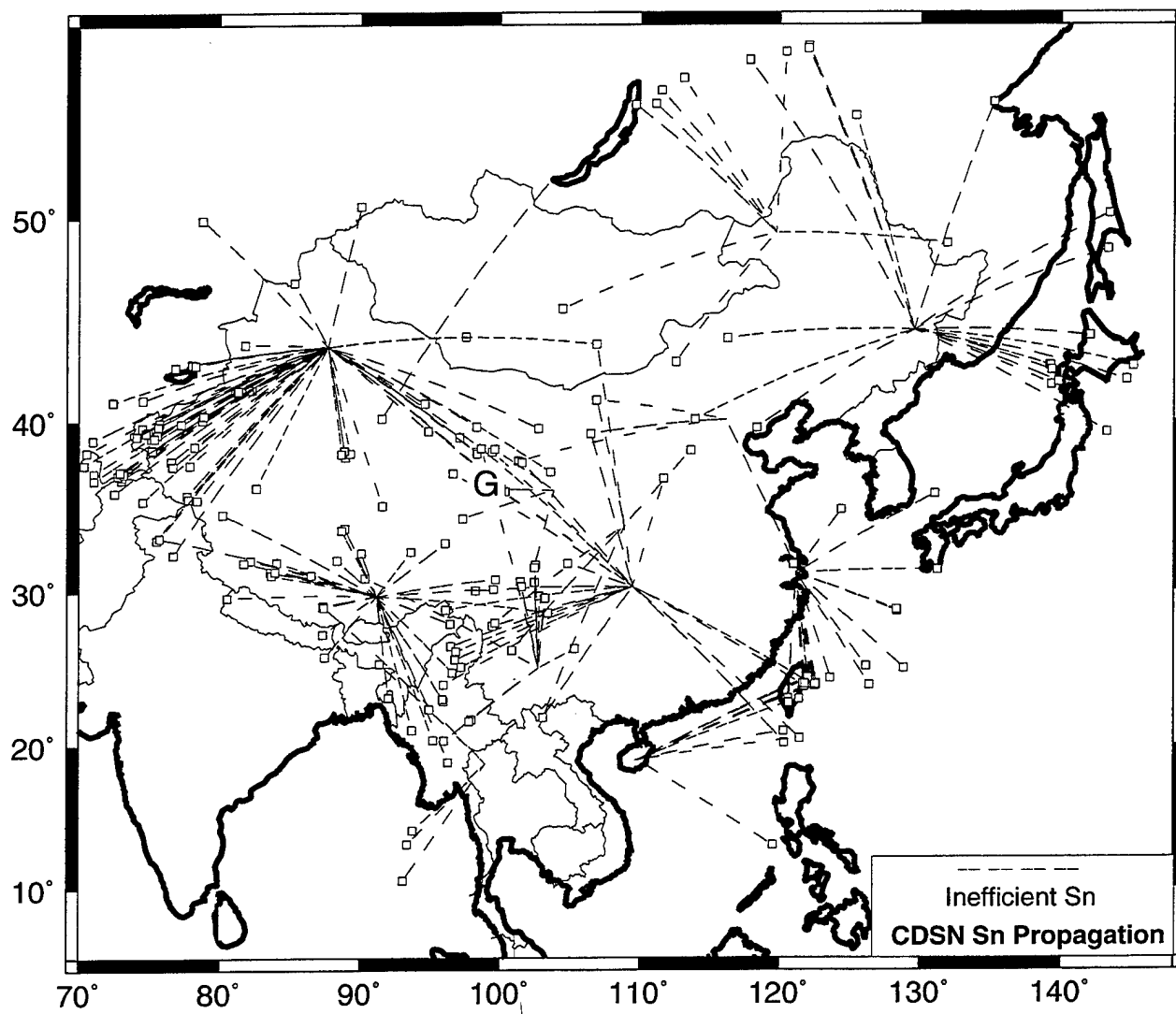Figure 10. A map of efficient Lg propagation paths in China. Solid lines depict efficient Lg ray paths.

Figure 11. A map of inefficient Lg propagation paths in China. Dashed lines represent inefficient station-event paths.

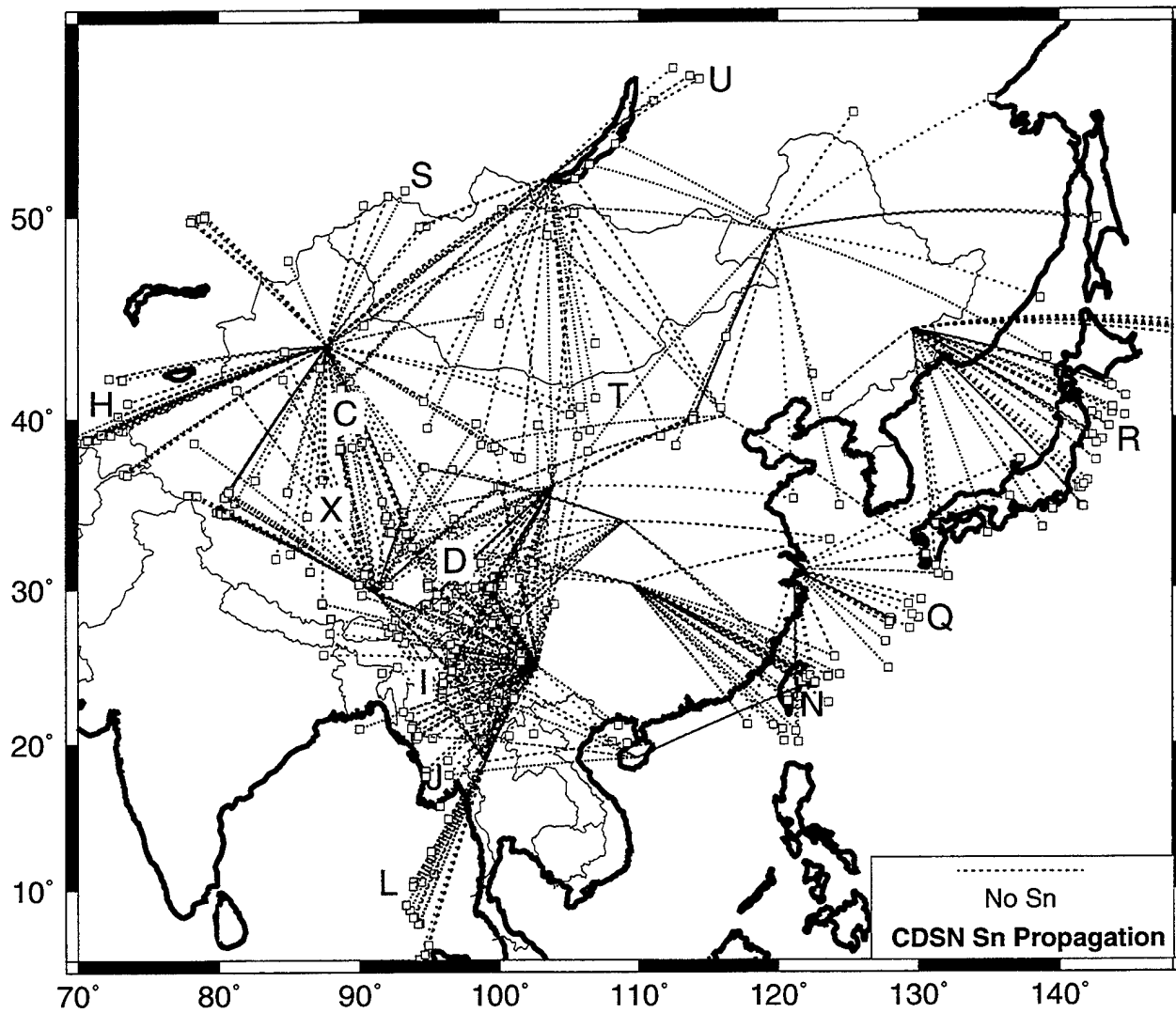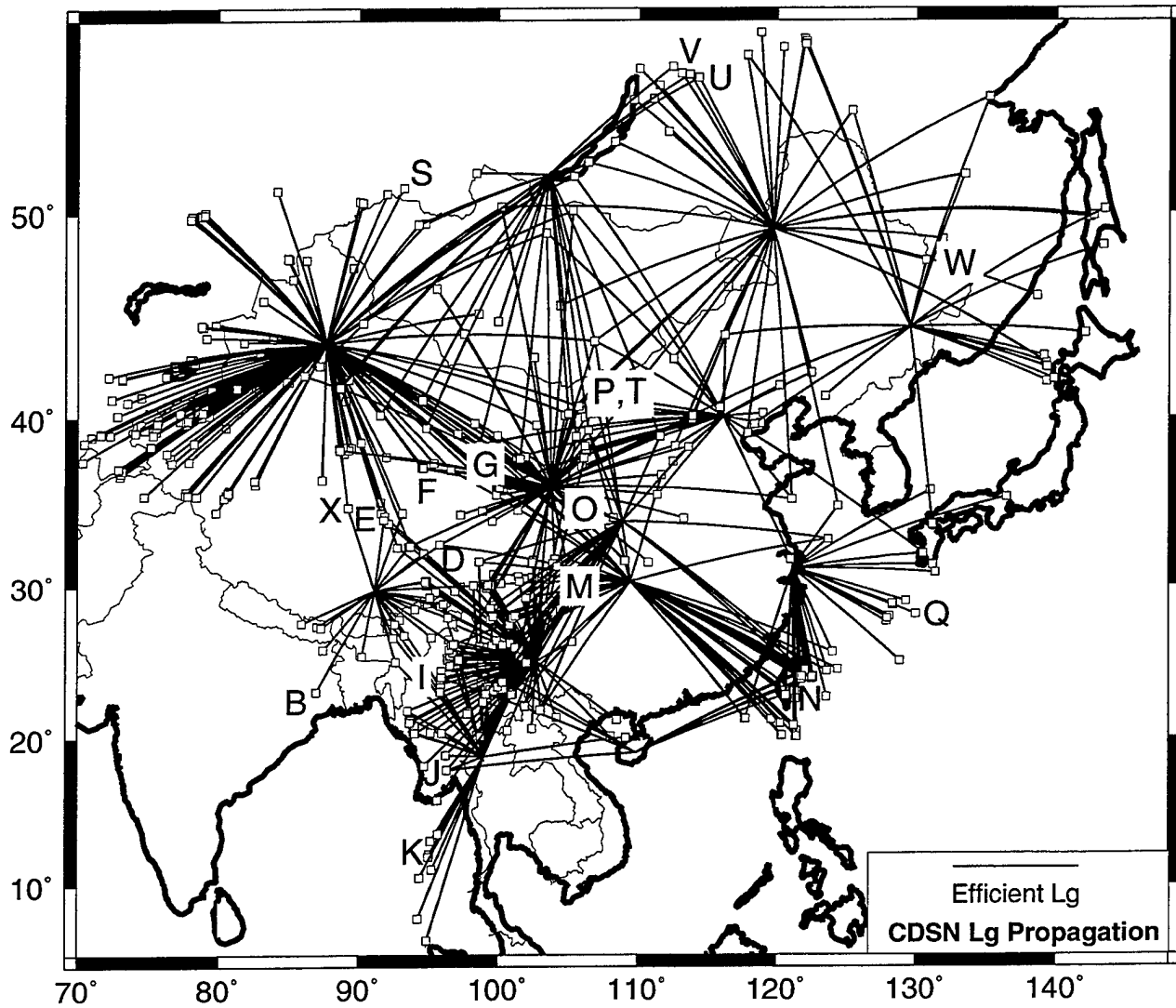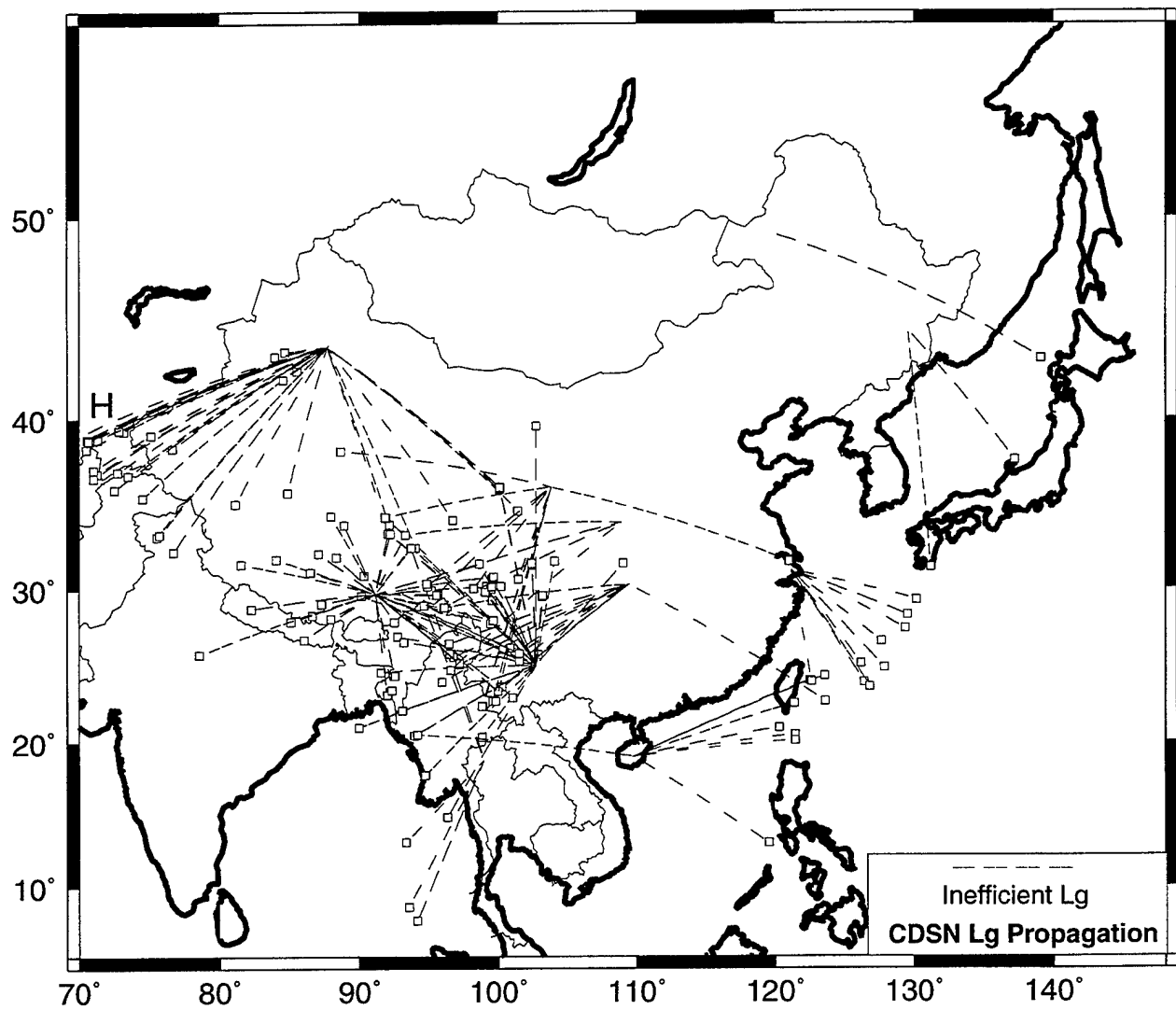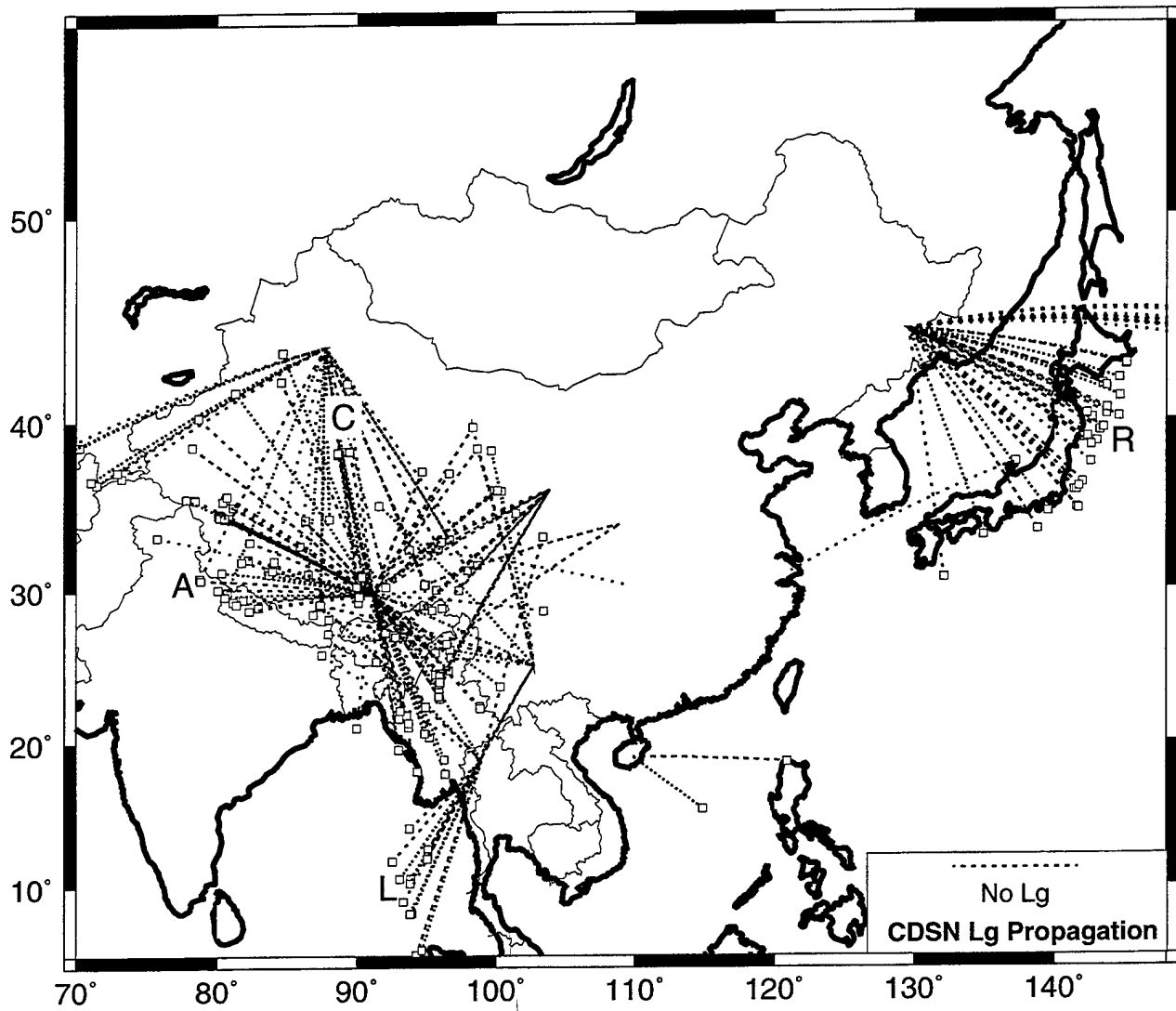Figure 12. A map depicting the propagation paths where Lg was completely eliminated or severely attenuated in China. Paths of Lg blockage are depicted by dotted lines.

Although Sn is highly attenuated through Mongolia and the Baikal Rift, strong Lg signals are recorded there (Figure 10, Seismograms S, T, and U). Lg is also seen for paths through the Tien Shan, Tarim Platform and Kunlun Fold System (Seismograms E, F, and G). Data from LZH also record efficient Lg through the Qinling Fold System (Seismogram O). Inefficient Lg may be seen for signals traveling from the Pamirs through the Tien Shan to WMQ (Seismogram H).

For a ray path from eastern Tibet to ENH, in central China, Lg is observed (Seismogram D). In southwest China, strong Lg waves are seen at KMI for paths traversing the Yangzi Paraplatform to the north and Burma to the west (Seismograms M and I, respectively). Efficient Lg is seen at ENH for paths through southeast China from Taiwan (Seismogram N). Seismogram J shows that Lg propagates efficiently for a long path through northern Indochina to QIZ. In the Andaman Sea, a ray path 10^0 away crossing more than 100 km of oceanic crust does not transmit Lg but a path 6^0 away, with the same backazimuth and not crossing oceanic crust, does propagate Lg (Seismograms L and K, respectively). Lg may also be weakened on the longer path by a change in the crustal waveguide at the oceanic ridge located in the Andaman Sea.

Station SSE, on the east coast of China, records many earthquakes from the island arcs east of China's continental margin. Seismograms recorded at SSE from Ryukyu events show mostly efficient and sometimes inefficient Lg arrivals. Seismogram Q shows an efficient Lg phase from an event in the Ryukyu Arc which travels mainly on the continental shelf, i.e. no oceanic crust. In northern China at MDJ, Lg is significantly weakened as it crosses the oceanic basin of the Sea of Japan (Seismogram R). Efficient Lg paths do cross the northern Sea of Japan from events in southern Hokkaido. However, these paths do not cross a significant amount of oceanic basin. Further inland, Lg has very large amplitudes on seismograms collected at station HIA (Seismograms V and W). These seismograms from HIA are from paths traversing the Argun and Da Hinggan Fold Systems. Figure 5 provides event data for three nuclear explosions and two earthquakes. Prominent, high-frequency Lg arrivals are seen on the explosion records (Seismograms a, b, and d). There are two earthquakes shown which are in the vicinity of the Lop Nor nuclear test site (Seismograms c and e). A visual inspection of these seismograms shows that the Lg/P amplitude ratios for the explosions are far larger than the ratios for the earthquakes. The Lg coda of the explosions also seems to be stronger and last longer than the coda for the earthquakes (Figure 5).

5. Discussion

The geological environment of China varies from stable continental shields to active/reactivated mountain belts, rifts and plateaus. As a result of the diversity of the regional geology, the high-frequency phases Sn and Lg show great lateral variability. Summary maps of Sn and Lg propagation efficiencies have provided insight into the crustal and mantle properties of the region and, when combined with existing geological information, into the explanation of why these phases are attenuated. Figure 13 is a summary map showing the major regions of efficient, inefficient and no Sn propagation. Figure 14 is a similar summary map of Lg propagation. Strong Sn waves are observed in the Tien Shan, Tarim Platform, southern Tibet, Yangzi Paraplatform and the Sino-Korean Platform. Efficient transmission is the expected result when propagation paths traverse stable shield regions. Inefficient Sn propagation is found in Western Tien Shan, southwest China and South China Sea. Sn attenuation or blockage occurs in north-central Tibet, the Japan and Ryukyu Arcs, Mongolia, the Baikal Rift and Burma. The strong Sn attenuation we observe on seismograms can be explained by a low-Q upper mantle due to partial melt. Partial melt may result from an enriched or refractory mantle caused by past subduction events as well as high temperatures. Water and sediments contained within the subducted lithosphere increase the amount of crustal material in the mantle of the back-arc region. When this subducted material is subjected to the right pressure-temperature conditions, water will be released into the mantle. This process will enhance partial melt by effectively lowering the solidus temperature. This interpretation, which was applied to the Iranian Plateau by Hearn and Ni (1994) and Rodgers et al. (1997), may explain the uppermost mantle in Burma, the Ryukyu and Japan Arcs, and Mongolia. The presence of Neogene alkali basaltic volcanism suggests that the upper mantle beneath Mongolia was hot at least in the recent past (Tapponnier and Molnar, 1979). In terms of island arc subduction, some work has found that Sn does not propagate on the concave side of island arcs due to a discontinuous high-Q upper mantle layer (e.g., McKenzie and Sclater, 1968; Molnar and Oliver, 1969). We have confirmed this result by our observation of Sn attenuation near island arc subduction in Burma and the Ryukyu and Japan Arcs. The spatial relationship between attenuation and volcanism in these island arc regions is consistent with the presence of partial melt in the uppermost mantle, which would account for the Sn attenuation. In the Baikal Rift region, evidence suggests there is a doming of the lithosphere on top of hot upwelling asthenospheric material (e.g., Gao et al., 1994; Logatchev and Florensov, 1978). This material in the lithospheric mantle would
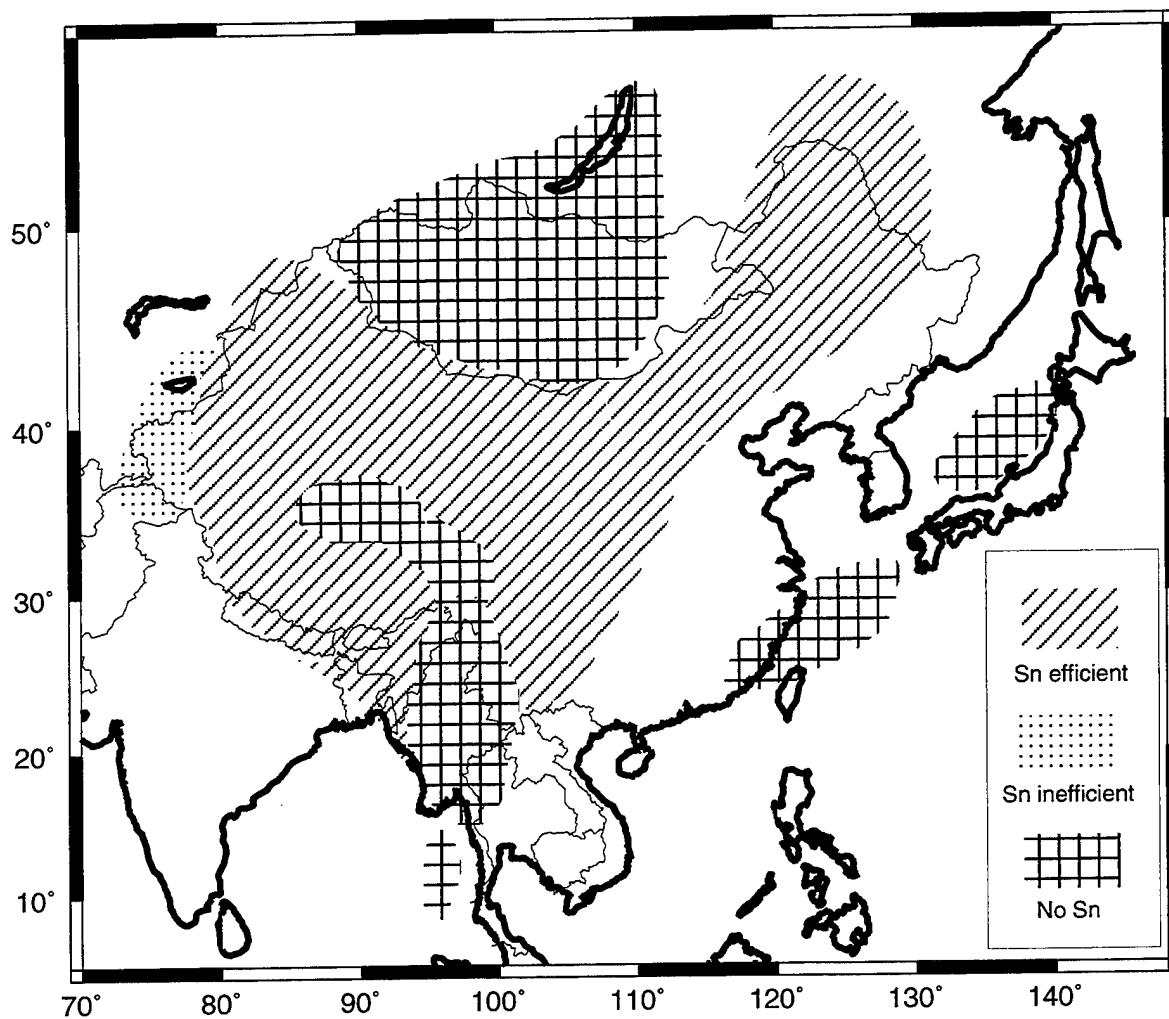
22

Figure 13. This is a summary map depicting the approximate regions of efficient, inefficient and no Sn propagation in the area of study. These are based on gross characteristics and are not definitive boundaries.
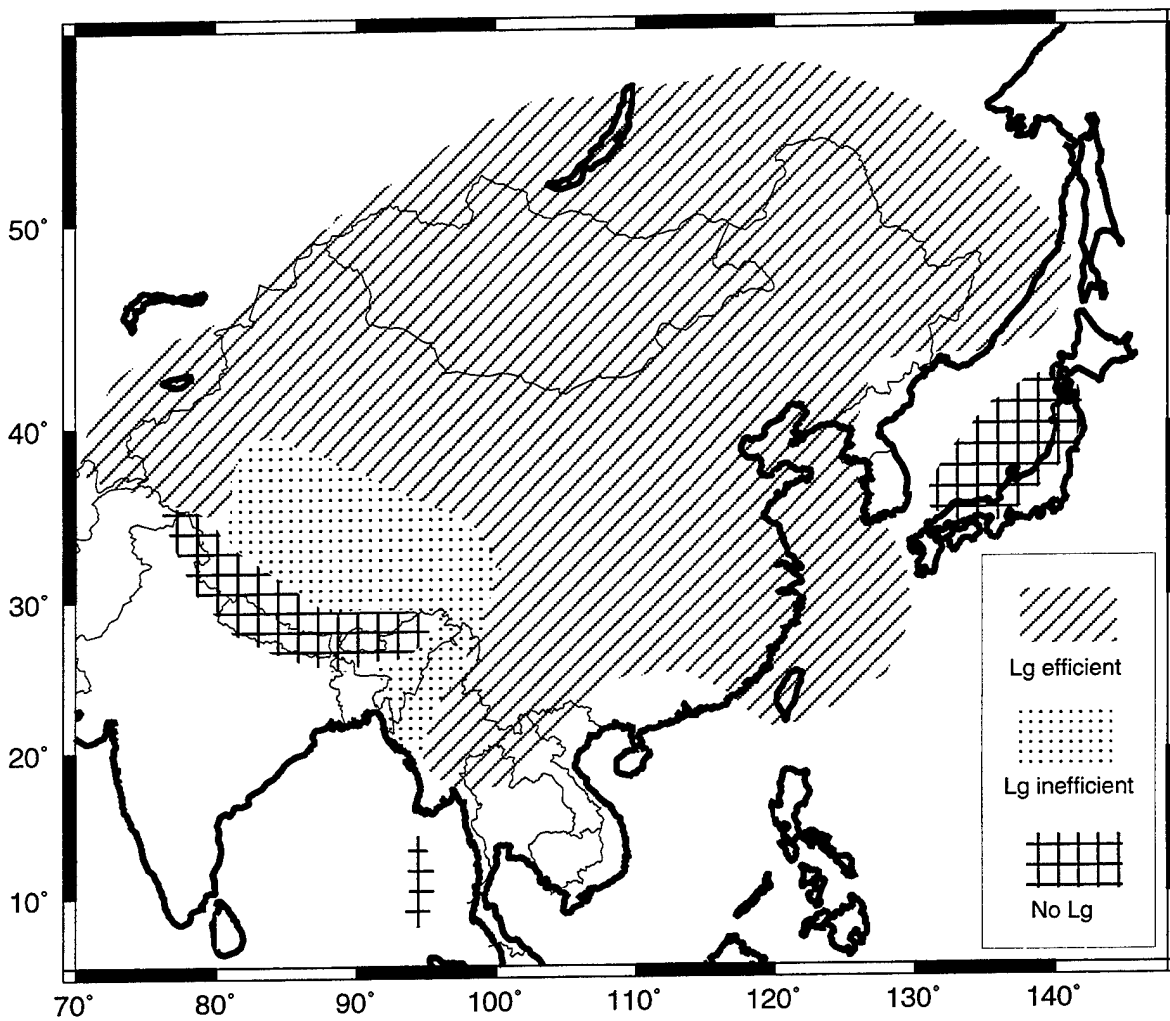
23

Figure 14. A summary map for efficient, inefficient and no Lg propagation in China and its surrounding regions.

severely attenuate Sn phases. In north-central Tibet, McNamara *et al.* (1995) argue that partial melt in the uppermost mantle explains why there is inefficient Sn but no comparable Pn attenuation. Previous studies in Tibet attributed elevated temperatures and low-Q values to Quartenary to Recent basaltic volcanism from an upper mantle source (e.g., Ni and Barazangi, 1983; Sengor and Kidd, 1979; Turner *et al.*, 1993).

Efficient Lg signals are observed throughout most of China (Figure 14). More specific, strong Lg energy is recorded for propagation paths crossing the Tien Shan, Tarim Platform, Yangzi Paraplatform, Burma, Mongolia and Sino-Korean Platform. Regions of inefficient Lg are limited mostly to northern Burma, central Tibet and the Pamirs. Lg blockage or partial blockage occurred for paths originating from the Japan Arc and Andaman Sea and for the southern boundary of the Tibetan Plateau (Figure 14). Lg is not expected to propagate for paths traversing oceanic crust in regions such as the Sea of Japan and Andaman Sea. This study could not resolve to what extent the islands of Japan themselves had on Lg propagation. Crustal structure and thickness variations on the boundaries of Tibet partially block Lg energy. The abrupt changes in crustal thickness in western China and Tibet may vary from 40 to 70 km depth over distances spanning less than a few hundred kilometers. Lg will propagate efficiently within Tibet for distances less than 6^0 away from station LSA (Figure 10, Seismogram W), but for longer distances within the plateau, Lg is weakened. The attenuation characteristics of southern Tibet were quantified by Reese and Ni (1996). They found a Q_c of approximately 150 at 1 Hz which is consistent with the existence of a low velocity zone in the mid-crust beneath the plateau. This suggests that high intrinsic attenuation in the crust is an important factor in the elimination of Lg as well as changes in the waveguide and the crustal structure.

This data set has not been used to rigorously constrain the boundaries between efficient and inefficient Sn and Lg propagation since the spatial resolution was not good enough to make constraints and several regions had overlapping efficiencies. We did, however, successfully map the gross propagation characteristics of these phases. This paper does have relevance to the application and monitoring of a CTBT in China by increasing the ground truth data in this large region and locating areas where regional seismic phases are partially blocked or attenuated. A high-frequency Sn discriminant would not be useful in a majority of China and its surrounding regions because of attenuation associated with the phase (Figure 13). Even in regions where Sn is efficient, it is usually only for short regional distances (5-8^0). On the other hand, Lg is very efficient in most

parts of China and outlying regions. Lg is blocked only for those paths crossing oceanic crust and for paths within and around the Tibetan Plateau. Currently, short-period ratios, which utilize the Lg arrival, are being developed for use in western China (e.g., Hartse *et al.*, 1996). Information learned from this study should help in the development of discriminants and ratio methods elsewhere in China, Indochina and Mongolia.

6. Conclusion

This investigation has increased our knowledge of the crust and uppermost mantle beneath China. It is evident that the complex geological and tectonic history of China has played a major role in the propagation characteristics of regional, high-frequency seismic phases. Partial melt in the upper mantle beneath island arc regions and locations of previous subduction events attenuates Sn signals. In this respect, the mantle in some regions of China may be analogous to the mantle beneath the Turkish-Iranian Plateau (e.g., Kadinsky-Cade *et al.*, 1981; Rodgers *et al.*, 1997). Volcanism in north-central Tibet and in the Mongolian Plateau provides evidence that the upper mantle beneath them is hot and partially melted and explains why Sn does not propagate through the regions. Another observation is that Lg is blocked when it travels across oceanic crust for more than a few hundred kilometers. It is also completely eliminated by abrupt crustal thickness changes and a partially melted, low-Q crust in Tibet. This study has shown that high Sn attenuation makes use of this phase difficult for nuclear discrimination; however, Lg could be an effective short-period nuclear discriminant in most of China with adequate station coverage.

7. References

Bath, M. (1966). Propagation of Sn and Pn to teleseismic distances, *Geofis. Pura Appl.* **64**, 19-30.

Bouchon, M. (1982). The complete synthesis of seismic crustal phases at regional distances, *J. Geophys. Res.* **78**, 1735-1741.

Brune, J. and J. Dorman (1963). Seismic waves and earth structure in the Canadian Shield, *Bull. Seism. Soc. Am.* **53**, 167-210.

Campillo, M. (1987). Lg wave propagation in a laterally varying crust and the spatial distribution of the quality factor in central France, *J. Geophys. Res.* **92**, 12604-12614.

Chinese Academy of Geological Sciences (1976). Map of tectonic systems of the People's Republic of China (in Chinese), Cartographic Publishing House, Beijing, 1:4,000,000.

Coleman, R. G. (1989). Continental growth of northwest China, *Tectonics* **8**, 621-635.

Gao, S., P. M. Davis, H. Liu, P. Slack, Y. A. Zorin, N. A. Logatchev, M. Kogan, P. Burkholder, and R. P. Meyer (1994). Asymmetric upwarp of the Asthenosphere beneath the Baikal rift zone, Siberia, *J. Geophys. Res.* **99**, 15319-15330.

Hartse, H. E., S. R. Taylor, W. S. Phillips, and G. E. Randall (1996). A preliminary study of regional seismic discrimination in central Asia with emphasis on western China, *Bull. Seism. Soc. Am.*, submitted.

Hearn, T. and J. Ni (1994). Pn velocities beneath continental collision zones: the Turkish-Iranian Plateau, *Geophys. J. Int.* **117**, 273-283.

Huang, J. (1979). Tectonic map of China, scale 1:4,000,000 (in Chinese), Cartographic Publishing House, Beijing.

Huang, J., R. Jishuan, J. Chunfa, Z. Zhengkun, and Q. Deyu (1987). Geotectonic evolution of China, Science Press, Beijing, and Springer-Verlag, Berlin, 214 pp.

Husebye, E. S. and B. O. Ruud (1996). Wave propagation in a complex crust - CTBT implications, *Proceeding of the 18th Annual Seismic Research Symposium on Monitoring a Comprehensive Test Ban Treaty*, Phillips Laboratory, 172-181, PL-TR-96-2153, ADA313692.

Kadinsky-Cade, K., M. Barazangi, J. Oliver, and B. Isacks (1981). Lateral Variations of high frequency seismic wave propagation at regional distances across the Turkish and Iranian Plateaus, *J. Geophys. Res.* **86**, 9377-9396.

Kennett, B. L. N. (1985). On Regional S, *Bull. Seism. Soc. Am.* **75**, 1077-1086.

Knopoff, L., F. Schwab, and E. Kausel (1973). Interpretation of Lg, *Geophys. J. R. Astr. Soc.* **33**, 389-404.

Liu, D. Y., A. P. Nutman, W. Compton, J. S. Wu, and Q. H. Shen (1992). Remnants of > 3800 Ma crust in the Chinese part of the Sino-Korean craton, *Geology* **20**, 339-342.

Logatchev, N. A. and N. A. Florensov (1978). The Baikal system of rift valleys, in N. A. Logatchev, and P. A. Mohr (editors), Geodynamics of the Baikal rift zone, *Tectonophysics* **45**, 1-13.

McKenzie, D. P. and J. G. Sclater (1968). Heat flow inside the island arcs of the northwestern Pacific, *J. Geophys. Res.* **73**, 3173-3179.

McNamara, D. E., T. J. Owens, and W. R. Walter (1995). Observations of regional phase propagation across the Tibetan Plateau, *J. Geophys. Res.* **100**, 22215-22229.

McNamara, D. E., T. J. Owens, and W. R. Walter, Propagation Characteristics of Lg across the Tibetan Plateau, *Bull. Seism. Soc. Am.*, in press.

Menke, W. H. and P. G. Richards (1980). Crust-mantle whispering gallery phases: a deterministic model of teleseismic Pn wave propagation, *J. Geophys. Res.* **185**, 5416-5422.

Molnar, P. and P. Tapponnier (1975). Cenezoic Tectonics of Asia: Effects of a Continental Collision, *Science* **189**, 419-426.

Molnar, P. and J. Oliver (1969). Lateral variations of attenuation in the upper mantle and discontinuities in the lithosphere, *J. Geophys. Res.* **74**, 2648-2682.

Ni, J. and M. Barazangi (1983). Velocities and propagation characteristics of Pn, Pg, Sn and Lg seismic waves beneath the Indian Shield, Himalayan Arc, Tibetan Plateau, and surrounding regions: High uppermost mantle velocities and efficient Sn propagation beneath Tibet, *Geophys. J. R. Astr. Soc.* **72**, 665-689.

Oliver, J. and M. Ewing (1958). Normal Modes of Continental Surface Waves, *Bull. Seism. Soc. Am.* **48**, 33-49.

Pomeroy, P. W., W. J. Best, and T. V. McEvilly (1982). Test ban treaty verification with regional data--a review, *Bull. Seism. Soc. Am.* **72**, S89-S129.

Press, F. and M. Ewing (1952). Two Slow Surface Waves Across North America, *Bull. Seism. Soc. Am.* **42**, 219-228.

Rodgers, A., J. Ni, and T. Hearn (1996). Pn, Sn, and Lg propagation in the Middle East, *Bull. Seism. Soc. Am.*, submitted.

Ruzaikin, A., I. Nersesov, V. Khalturin, and P. Molnar (1977). Propagation of Lg and lateral variations in crustal structure in Asia, *J. Geophys. Res.* **82**, 307-316.

Sengor, A. M. C. and W. S. F. Kidd (1979). Post-collisional tectonics of the Turkish-Iranian Plateau and a comparison with Tibet, *Tectonophysics* **55**, 361-376.

Sengor, A. M. C. (1987). Tectonic subdivision and evolution of Asia, *Bull. Tech. Univ. Istanbul* **40**, 355-435.

Stephens, C. and B. Isacks (1977). Toward an understanding of Sn: normal modes of Love waves in an oceanic structure, *Bull. Seism. Soc. Am.* **67**, 69-78.

Tapponnier, P. and P. Molnar (1979). Active faulting and Cenezoic tectonics of the Tien Shan, Mongolia, and Baykal regions, *J. Geophys. Res.* **84**, 3425-3459.

Taylor S. R., M. D. Denny, E. S. Vergino, and R. E. Glaser (1989). Regional discrimination between NTS explosions and earthquakes, *Bull. Seism. Soc. Am.* **79**, 1142-1176.

Turner, S., C. Hawkesworth, J. Liu, N. Rodgers, S. Kelley, and P. VanCalsteren (1993). Timing of Tibetan uplift constrained by analysis of volcanic rocks, *Nature* **364**, 50-54.

Yin, A. and S. Nie (1996). A Phanerozoic palinspastic reconstruction of China and its neighboring regions, in A. Yin and M. Harrison (editors), The Tectonic Evolution of Asia, Cambridge University Press, 442-485.

THOMAS AHRENS
SEISMOLOGICAL LABORATORY 252-21
CALIFORNIA INSTITUTE OF TECHNOLOGY
PASADENA, CA 91125

RALPH ALEWINE
NTPO
1901 N. MOORE STREET, SUITE 609
ARLINGTON, VA 22209

SHELTON ALEXANDER
PENNSYLVANIA STATE UNIVERSITY
DEPARTMENT OF GEOSCIENCES
537 DEIKE BUILDING
UNIVERSITY PARK, PA 16801

MUAWIA BARAZANGI
INSTITUTE FOR THE STUDY OF THE CONTINENTS
3126 SNEE HALL
CORNELL UNIVERSITY
ITHACA, NY 14853

T.G. BARKER
MAXWELL TECHNOLOGIES
8888 BALBOA AVE.
SAN DIEGO, CA 92123-1506

DOUGLAS BAUMGARDT
ENSCO INC.
5400 PORT ROYAL ROAD
SPRINGFIELD, VA 22151

THERON J. BENNETT
MAXWELL TECHNOLOGIES
11800 SUNRISE VALLEY DRIVE SUITE 1212
RESTON, VA 22091

WILLIAM BENSON
NAS/COS
ROOM HA372
2001 WISCONSIN AVE. NW
WASHINGTON, DC 20007

JONATHAN BERGER
UNIVERSITY OF CA, SAN DIEGO
SCRIPPS INSTITUTION OF OCEANOGRAPHY IGPP, 0225
9500 GILMAN DRIVE
LA JOLLA, CA 92093-0225

ROBERT BLANDFORD
AFTAC
1300 N. 17TH STREET
SUITE 1450
ARLINGTON, VA 22209-2308

STEVEN BRATT
NTPO
1901 N. MOORE STREET, SUITE 609
ARLINGTON, VA 22209

RHETT BUTLER
IRIS
1200 NEW YORK AVE., NW
SUITE 800
WASHINGTON, DC 20005

LESLIE A. CASEY
DOE
1000 INDEPENDENCE AVE. SW
NN-20
WASHINGTON, DC 20585-0420

CATHERINE DE GROOT-HEDLIN
UNIVERSITY OF CALIFORNIA, SAN DIEGO
INSTITUTE OF GEOPHYSICS AND PLANETARY PHYSICS
8604 LA JOLLA SHORES DRIVE
SAN DIEGO, CA 92093

STANLEY DICKINSON
AFOSR
110 DUNCAN AVENUE, SUITE B115
BOLLING AFB
WASHINGTON, D.C. 20332-001

DIANE I. DOSER
DEPARTMENT OF GEOLOGICAL SCIENCES
THE UNIVERSITY OF TEXAS AT EL PASO
EL PASO, TX 79968

RICHARD J. FANTEL
BUREAU OF MINES
DEPT OF INTERIOR, BLDG 20
DENVER FEDERAL CENTER
DENVER, CO 80225

MARK D. FISK
MISSION RESEARCH CORPORATION
735 STATE STREET
P.O. DRAWER 719
SANTA BARBARA, CA 93102-0719

ROBERT GEIL
DOE
PALAIS DES NATIONS, RM D615
GENEVA 10, SWITZERLAND

LORI GRANT
MULTIMAX, INC.
311C FOREST AVE. SUITE 3
PACIFIC GROVE, CA 93950

1

HENRY GRAY
SMU STATISTICS DEPARTMENT
P.O. BOX 750302
DALLAS, TX 75275-0302

DAVID HARKRIDER
PHILLIPS LABORATORY
EARTH SCIENCES DIVISION
29 RANDOLPH ROAD
HANSCOM AFB, MA 01731-3010

THOMAS HEARN
NEW MEXICO STATE UNIVERSITY
DEPARTMENT OF PHYSICS
LAS CRUCES, NM 88003

DONALD HELMBERGER
CALIFORNIA INSTITUTE OF TECHNOLOGY
DIVISION OF GEOLOGICAL & PLANETARY SCIENCES
SEISMOLOGICAL LABORATORY
PASADENA, CA 91125

ROBERT HERRMANN
ST. LOUIS UNIVERSITY
DEPARTMENT OF EARTH & ATMOSPHERIC SCIENCES
3507 LACLEDE AVENUE
ST. LOUIS, MO 63103

ANTHONY IANNACCHIONE
BUREAU OF MINES
COCHRANE MILL ROAD
PO BOX 18070
PITTSBURGH, PA 15236-9986

THOMAS JORDAN
MASSACHUSETTS INSTITUTE OF TECHNOLOGY
EARTH, ATMOSPHERIC & PLANETARY SCIENCES
77 MASSACHUSETTS AVENUE, 54-918
CAMBRIDGE, MA 02139

LAWRENCE LIVERMORE NATIONAL LABORATORY
ATTN: TECHNICAL STAFF (PLS ROUTE)
PO BOX 808, MS L-221
LIVERMORE, CA 94551

LAWRENCE LIVERMORE NATIONAL LABORATORY
ATTN: TECHNICAL STAFF (PLS ROUTE)
PO BOX 808, MS L-208
LIVERMORE, CA 94551

LAWRENCE LIVERMORE NATIONAL LABORATORY
ATTN: TECHNICAL STAFF (PLS ROUTE)
PO BOX 808, MS L-195
LIVERMORE, CA 94551

I. N. GUPTA
MULTIMAX, INC.
1441 MCCORMICK DRIVE
LARGO, MD 20774

IAN MACGREGOR
NSF
4201 WILSON BLVD., ROOM 785
ARLINGTON, VA 22230

MICHAEL HEDLIN
UNIVERSITY OF CALIFORNIA, SAN DIEGO
SCRIPPS INSTITUTION OF OCEANOGRAPHY IGPP, 0225
9500 GILMAN DRIVE
LA JOLLA, CA 92093-0225

EUGENE HERRIN
SOUTHERN METHODIST UNIVERSITY
DEPARTMENT OF GEOLOGICAL SCIENCES
DALLAS, TX 75275-0395

VINDELL HSU
HQ/AFTAC/TTR
1030 S. HIGHWAY A1A
PATRICK AFB, FL 32925-3002

RONG-SONG JIH
HQ DSWA/PMP/CTBT
6801 TELEGRAPH ROAD
ALEXANDRIA, VA 22310-3398

LAWRENCE LIVERMORE NATIONAL LABORATORY
ATTN: TECHNICAL STAFF (PLS ROUTE)
PO BOX 808, MS L-200
LIVERMORE, CA 94551

LAWRENCE LIVERMORE NATIONAL LABORATORY
ATTN: TECHNICAL STAFF (PLS ROUTE)
LLNL
PO BOX 808, MS L-175
LIVERMORE, CA 94551

LAWRENCE LIVERMORE NATIONAL LABORATORY
ATTN: TECHNICAL STAFF (PLS ROUTE)
PO BOX 808, MS L-202
LIVERMORE, CA 94551

LAWRENCE LIVERMORE NATIONAL LABORATORY
ATTN: TECHNICAL STAFF (PLS ROUTE)
PO BOX 808, MS L-205
LIVERMORE, CA 94551

THORNE LAY
UNIVERSITY OF CALIFORNIA, SANTA CRUZ
EARTH SCIENCES DEPARTMENT
EARTH & MARINE SCIENCE BUILDING
SANTA CRUZ, CA 95064

ANATOLI L. LEVSHIN
DEPARTMENT OF PHYSICS
UNIVERSITY OF COLORADO
CAMPUS BOX 390
BOULDER, CO 80309-0309

DONALD A. LINGER
DNA
6801 TELEGRAPH ROAD
ALEXANDRIA, VA 22310

LOS ALAMOS NATIONAL LABORATORY
ATTN: TECHNICAL STAFF (PLS ROUTE)
PO BOX 1663, MS F659
LOS ALAMOS, NM 87545

LOS ALAMOS NATIONAL LABORATORY
ATTN: TECHNICAL STAFF (PLS ROUTE)
PO BOX 1663, MS F665
LOS ALAMOS, NM 87545

LOS ALAMOS NATIONAL LABORATORY
ATTN: TECHNICAL STAFF (PLS ROUTE)
PO BOX 1663, MS D460
LOS ALAMOS, NM 87545

LOS ALAMOS NATIONAL LABORATORY
ATTN: TECHNICAL STAFF (PLS ROUTE)
PO BOX 1663, MS C335
LOS ALAMOS, NM 87545

GARY MCCARTOR
SOUTHERN METHODIST UNIVERSITY
DEPARTMENT OF PHYSICS
DALLAS, TX 75275-0395

KEITH MCLAUGHLIN
MAXWELL TECHNOLOGIES
8888 BALBOA AVE.
SAN DIEGO, CA 92123-1506

BRIAN MITCHELL
DEPARTMENT OF EARTH & ATMOSPHERIC SCIENCES
ST. LOUIS UNIVERSITY
3507 LACLEDE AVENUE
ST. LOUIS, MO 63103

RICHARD MORROW
USACDA/IVI
320 21ST STREET, N.W.
WASHINGTON, DC 20451

JOHN MURPHY
MAXWELL TECHNOLOGIES
11800 SUNRISE VALLEY DRIVE SUITE 1212
RESTON, VA 22091

JAMES NI
NEW MEXICO STATE UNIVERSITY
DEPARTMENT OF PHYSICS
LAS CRUCES, NM 88003

JOHN ORCUTT
INSTITUTE OF GEOPHYSICS AND PLANETARY PHYSICS
UNIVERSITY OF CALIFORNIA, SAN DIEGO
LA JOLLA, CA 92093

PACIFIC NORTHWEST NATIONAL LABORATORY
ATTN: TECHNICAL STAFF (PLS ROUTE)
PO BOX 999, MS K6-48
RICHLAND, WA 99352

PACIFIC NORTHWEST NATIONAL LABORATORY
ATTN: TECHNICAL STAFF (PLS ROUTE)
PO BOX 999, MS K6-40
RICHLAND, WA 99352

PACIFIC NORTHWEST NATIONAL LABORATORY
ATTN: TECHNICAL STAFF (PLS ROUTE)
PO BOX 999, MS K6-84
RICHLAND, WA 99352

PACIFIC NORTHWEST NATIONAL LABORATORY
ATTN: TECHNICAL STAFF (PLS ROUTE)
PO BOX 999, MS K5-12
RICHLAND, WA 99352

FRANK PILOTTE
HQ/AFTAC/TT
1030 S. HIGHWAY A1A
PATRICK AFB, FL 32925-3002

KEITH PRIESTLEY
DEPARTMENT OF EARTH SCIENCES
UNIVERSITY OF CAMBRIDGE
MADINGLEY RISE, MADINGLEY ROAD
CAMBRIDGE, CB3 OEZ UK

JAY PULLI
BBN
1300 NORTH 17TH STREET
ROSSLYN, VA 22209

PAUL RICHARDS
COLUMBIA UNIVERSITY
LAMONT-DOHERTY EARTH OBSERVATORY
PALISADES, NY 10964

DAVID RUSSELL
HQ AFTAC/TTR
1030 SOUTH HIGHWAY A1A
PATRICK AFB, FL 32925-3002

CHANDAN SAIKIA
WOOODWARD-CLYDE FEDERAL SERVICES
566 EL DORADO ST., SUITE 100
PASADENA, CA 91101-2560

SANDIA NATIONAL LABORATORY
ATTN: TECHNICAL STAFF (PLS ROUTE)
DEPT. 5704
MS 0979, PO BOX 5800
ALBUQUERQUE, NM 87185-0979

SANDIA NATIONAL LABORATORY
ATTN: TECHNICAL STAFF (PLS ROUTE)
DEPT. 5791
MS 0567, PO BOX 5800
ALBUQUERQUE, NM 87185-0567

SANDIA NATIONAL LABORATORY
ATTN: TECHNICAL STAFF (PLS ROUTE)
DEPT. 9311
MS 1159, PO BOX 5800
ALBUQUERQUE, NM 87185-1159

SANDIA NATIONAL LABORATORY
ATTN: TECHNICAL STAFF (PLS ROUTE)
DEPT. 5704
MS 0655, PO BOX 5800
ALBUQUERQUE, NM 87185-0655

SANDIA NATIONAL LABORATORY
ATTN: TECHNICAL STAFF (PLS ROUTE)
DEPT. 5736
MS 0655, PO BOX 5800
ALBUQUERQUE, NM 87185-0655

THOMAS SERENO JR.
SCIENCE APPLICATIONS INTERNATIONAL
CORPORATION
10260 CAMPUS POINT DRIVE
SAN DIEGO, CA 92121

AVI SHAPIRA
SEISMOLOGY DIVISION
THE INSTITUTE FOR PETROLEUM RESEARCH AND
GEOPHYSICS
P.O.B. 2286, NOLON 58122 ISRAEL

ROBERT SHUMWAY
410 MRAK HALL
DIVISION OF STATISTICS
UNIVERSITY OF CALIFORNIA
DAVIS, CA 95616-8671

MATTHEW SIBOL
ENSCO, INC.
445 PINEDA COURT
MELBOURNE, FL 32940

DAVID SIMPSON
IRIS
1200 NEW YORK AVE., NW
SUITE 800
WASHINGTON, DC 20005

JEFFRY STEVENS
MAXWELL TECHNOLOGIES
8888 BALBOA AVE.
SAN DIEGO, CA 92123-1506

BRIAN SULLIVAN
BOSTON COLLEGE
INSITUTE FOR SPACE RESEARCH
140 COMMONWEALTH AVENUE
CHESTNUT HILL, MA 02167

DAVID THOMAS
ISEE
29100 AURORA ROAD
CLEVELAND, OH 44139

NAFI TOKSOZ
EARTH RESOURCES LABORATORY, M.I.T.
42 CARLTON STREET, E34-440
CAMBRIDGE, MA 02142

LAWRENCE TURNBULL
ACIS
DCI/ACIS
WASHINGTON, DC 20505

GREG VAN DER VINK
IRIS
1200 NEW YORK AVE., NW
SUITE 800
WASHINGTON, DC 20005

5